SAE The Engineering Society For Advancing Mobility Land Sea Air and Space®
INTERNATIONAL

400 COMMONWEALTH DRIVE, WARRENDALE, PA 15096-0001 U.S.A.

SAE Technical Paper Series

902280

A Band Variable-Inertia Flywheel Integrated-Urban Transit Bus Performance

Hamid Moosavi-Rad
Dept. of Mechanical Engineering
Seattle University
David G. Ullman
Dept. of Mechanical Engineering
Oregon State University

Truck and Bus Meeting and Exposition
Detroit, Michigan
October 29 — November 1, 1990

902280

A Band Variable-Inertia Flywheel Integrated-Urban Transit Bus Performance

Hamid Moosavi-Rad
Dept. of Mechanical Engineering
Seattle University
David G. Ullman
Dept. of Mechanical Engineering
Oregon State University

Abstract

By means of computer simulation, the potential of a Band Variable-Inertia Flywheel (BVIF) as an energy storage device for a diesel engine city bus is evaluated. Replacing both a fixed-inertia flywheel (FIF) and a continuously variable transmission (CVT), the BVIF is capable of accelerating a vehicle from rest to a nearly-constant speed, while recovering part of the kinetic energy normally dissipated through braking of the vehicle.

The results are compared with that of conventionally-powered bus. A fuel saving of up to 30 percent is shown with the BVIF-integrated system. The regenerative braking system reduces brake wear by a factor of five in comparison with the conventional vehicle.

Introduction

As nonrenewable energy sources become more scarce, the concept of storing kinetic energy in a form in which it can be reused to improve the efficiency of a system is very attractive. One method in which kinetic energy can be stored or retained is in the rotational mass of a flywheel. Due to its very simple configuration, the flywheel has had many applications in the past and poses new possibilities for innovative use in the future.

This paper examines in depth, by means of computer simulation, the application of a band variable-inertia flywheel (BVIF) integrated into the drive and braking systems of an urban transit city bus to improve fuel consumption and overall performance of the vehicle.

Because of the nature of inner-city driving, these vehicles are constantly either accelerating or decelerating. Therein lies the problem. The highest power demand of these vehicles is during the course of acceleration.

However, these vehicles seldom reach constant cruising speed before they have to come to stop again. If the energy normally dissipated during the braking could be stored to be reused during the next course of acceleration, significant fuel savings may result. The regenerative braking system would also reduce the cost of routine maintenance and as a result extension of the life of the brake shoes.

To accomplish the above tasks, three alternative designs for the position of the BVIF within the vehicle are proposed. The best of these possible configurations is identified.

A Conventionally-Powered Transit Bus

For the purpose of this study, the most widely-used city bus, a Detroit Diesel Allison conventional passenger coach has been chosen for performance evaluation. The term "performance" refers to four major areas: acceleration, cruise, deceleration and fuel consumption. A mathematical model of the bus and a digital computer simulation examine the dynamics of these parameters over a prescribed terrain.

The data representing the physical dimensions of the bus, its engine characteristics, torque convertor and power transmission are provided by the manufacturers of these buses [1]. These data are used to evaluate the performance of the vehicle. This has been accomplished through Newton's Second Law of motion:

$$F_{sum} = M_{eq} * a \qquad (1)$$

where F_{sum} represents the summation of the forces acting on the vehicle, that is the driving forces from the prime mover, namely tractive force, the aerodynamic resistance, the rolling resistance and the weight of the vehicle as shown in Figure 1.

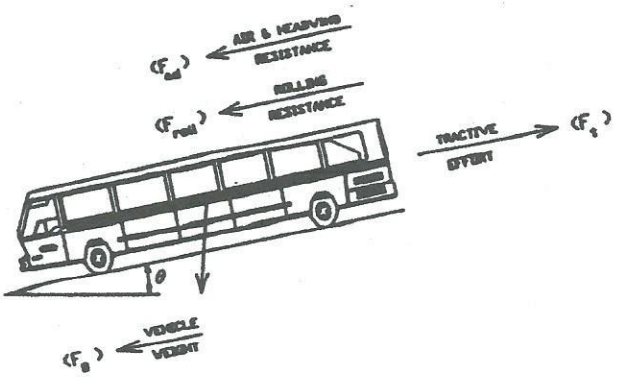

Figure 1 - Bus free body diagram

Driveline losses including the vehicle's torque convertor, power transmission and the axle shaft are taken into consideration when formulating the equation of motion of the vehicle. The term M_{eq} represents the effective mass of the vehicle which consist of the mass of the vehicle and the rotational inertia of the engine, the engine flywheel and the tries. The relatively small inertia of the propeller shaft, transmission gears and clutches, and rear axle is assumed to be negligible. The mathematical equation for the equivalent mass is in the following form [2]:

$$M_{eq} = \frac{W_{tot}}{g} + \frac{1}{r_{tire}^2}\left(I_{eng} * gr_{ovr}^2 + I_{tire}\right) \qquad (2)$$

where,

W_{tot} = total vehicle and passengers weight, lbf
r_{tire} = tire outer radius, ft
I_{eng} = engine, engine flywheel and clutches inertia, lbf-ft-sec^2
gr_{ovr} = overall gear ratio
I_{tire} = combined tire, wheel and brake drum inertia, lbf-ft-sec^2

Dynamic Modeling of the Vehicle Acceleration and Deceleration

A summary of the above description of the vehicle motion is simplified in the block diagram as shown in Figure 2. This diagram is based on the analytical equation which results in a nonlinear differential equation expressed in terms of the vehicle's velocity [3]. The net vehicle force available to the rear wheels is calculated by subtracting the resistance forces, aerodynamic friction, rolling friction and grade force, if any, from the tractive force provided by the vehicle engine. The vehicle acceleration is obtained by dividing the net force by the sum of the vehicle mass and effective inertia mass, namely equivalent mass.

Incrementing the velocity with a step size of one to two miles per hour, the elapsed time in each velocity increment and the distance traveled by the vehicle can then be calculated. A sample output of the bus performance is presented in later sections when the comparison is made with the BVIF-integrated bus performance.

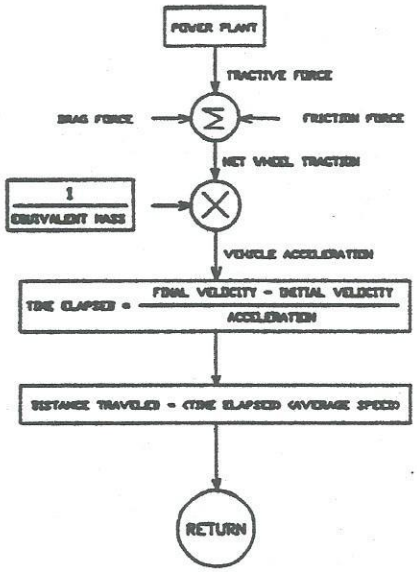

Figure 2 - Vehicle dynamic block diagram

Band Variable-Inertia Flywheel Geometry

This section presents a brief overview of the band variable-inertia flywheel configuration and dynamic modeling of the BVIF system.

The band variable-inertia flywheel is constructed of a hollow cylinder (the outer casing) and a rotational shaft (the inner hub) as shown in Figure 3 [4]. The means of connection between the outer casing and the inner hub is a thin flexible material, the band.

One end of the band is connected to the inner hub, while the opposite end is attached to the inner surface of the outer casing. The band will unwind from the inner hub and wind inside the outer casing depending upon their relative angular velocities. Fixing the inertia of the inner hub and the outer casing, any variation in the amount of the band

material wrapped around the hub will describe the change in the moment of inertia of the system, and

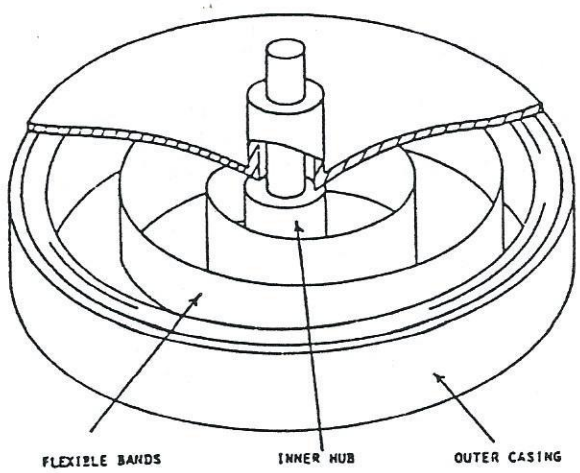

Figure 3 - The Band-Type Variable-Inertia Flywheel [4]

therefore the inertia characteristics of the BVIF. A detailed geometric analysis of the BVIF system is given by David G. Ullman [4].

Concept of Variable-Inertia Flywheel

Before discussing what the variable inertia flywheel is, the flywheel in its simple form, fixed-inertia is considered. In mathematical form, the kinetic energy stored into a flywheel, is in the following form:

$$E = \frac{1}{2} I \omega^2 \qquad (3)$$

where, I is the mass moment of inertia, and ω is the rotational angular velocity of the mass.

Varying the flywheel's rotational speed is the only means of changing the energy content of the system. As reduction in rotational rate causes energy to be released from the flywheel. As a load being powered by the flywheel normally requires a constant or even increasing rotational rate power source, this reduction in rotational speed is a distinct disadvantage. However, any continuously variable transmission (CVT) such as a traction drive, a hydraulic pump and pump and motor, or an electric generator and motor can be employed to compensate for this mismatch in rotational rate.

Extensive research has been conducted regarding the use of CVT as an intermediate means for transferring power from the flywheel to the prime load [5,6,7,8,9]. Yet, such systems still remain complex, inefficient, limited in power-handling capability, and costly.

Rather than the angular speed of the flywheel, an alternative method for storing and regaining energy content of the flywheel may exist and may be derived by reconsidering the equation for kinetic energy (Equation 3). This alternative achieves a change in energy by varying the flywheel's mass moment of inertia, rather than its angular speed [4,10,11,12,13].

Mass moment of inertia of a flywheel is a function of the mass and its effective radius from the rotational axis. It is expressed by the relation $I = \int r^2 \, dm$. Altering I requires that the geometry of the flywheel about the spin axis be variable, implying the existence of some moving components in the flywheel as its rotational rate changes. The resulting mechanism is the Variable-Inertia Flywheel (VIF).

In comparison to the fixed-inertia flywheel, the design of the variable-inertia flywheel will be by far more complicated and will result in a weight increase per unit-energy-stored relative to a comparable fixed-inertia design. However, if a VIF could replace both a FIF and a CVT, this weight gain due to addition of VIF system might still result in a much lighter system overall [10]. It is therefore possible to argue that a variable-inertia flywheel integrated into a vehicle for auxiliary energy storage could result in a lighter, less costly, and more efficient vehicle when compared to a similar model employing the conventional fixed-inertia flywheel.

Dynamic Modeling of the BVIF

In formulating the dynamics equation of motion for a BVIF, the Lagrange's Method is used [12]. As long as the BVIF rotates in a horizontal plane, the variation in the potential energy of the system is negligible. Therefore, the behavior of the system can best be explained when the kinetic energy is used as the primary base for evaluating the equations of motion.

Although there always exists a small portion of the band which is travelling both radially and rotationally as the band transfers between the inner hub and the outer casing, this amount of material seems negligible compared to the total mass of the band. Thus, the total kinetic energy of the system is described as:

$$KE = \frac{1}{2} I_i \omega_i^2 + \frac{1}{2} I_o \omega_o^2 \qquad (4)$$

where the subscripts i and o indicates the inner and outer segments of the BVIF. I_i and I_o include the fixed moment of inertia of the inner hub and the outer casing, as well as the corresponding band material inertia.

The generalized forces (torques) applied to each segment of the BVIF are expressed as two independent coordinates: θ_i of the inner hub and θ_o of

the outer casing. The following equations of motion describe the behavior of the system:

$$\frac{d}{dt}\frac{\partial KE}{\partial \dot{\theta}_i} - \frac{\partial KE}{\partial \theta_i} = \sum T_i \qquad (5)$$

$$\frac{d}{dt}\frac{\partial KE}{\partial \dot{\theta}_o} - \frac{\partial KE}{\partial \theta_o} = \sum T_o \qquad (6)$$

where $\sum T_i$ and $\sum T_o$ represent the resultant external torque contribution of the inner hub and the outer casing of the BVIF respectively. Due to the chronological variability of the inertias, the above relations are functions of the relationship among these four variables: I_i, ω_i, I_o, and ω_o.

The exact nature of the relationship among these four variables is dependent upon the manner of connection to and the characteristics of the system into which the band variable-inertia flywheel is integrated [12]. Performing the proper differentiations in Equations (5) and (6) yields the dynamic differential equation of motion that predict the behavior of the BVIF system.

BVIF Powering an Inertial Load

One manner in which the BVIF could be connected to an inertial load is through an intermediate planetary gear system [3] as shown in Figure 4 [14].

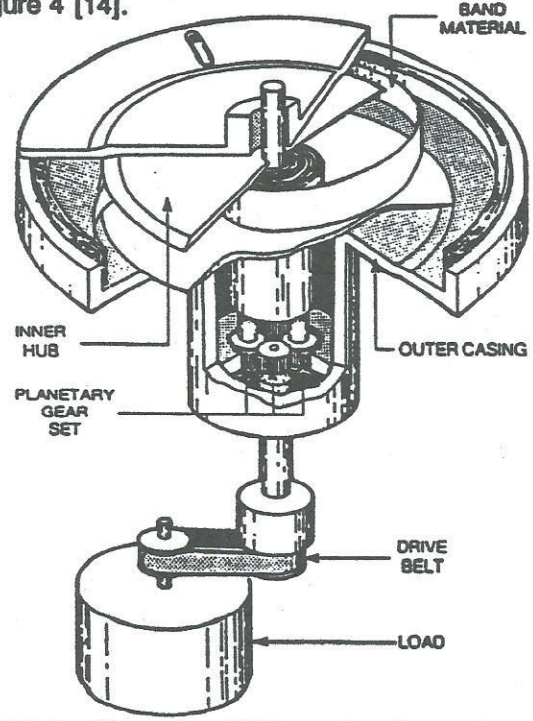

Figure 4 - Example of VIF accelerating an inertial load [14]

When the load is being accelerated, the inner hub is connected to the carrier arm of a planetary gear set and the outer casing to the ring gear, the inertial load is linked to the sun gear. This arrangement is shown in Figure 5 [3]. In this figure, the clutch C_i is connecting the BVIF inner hub to the carrier arm of the planetary gear set. The clutch C_o is the interconnection between the outer casing and the ring gear, and the sun gear of the planetary set engages with the inertial load through clutch C_L.

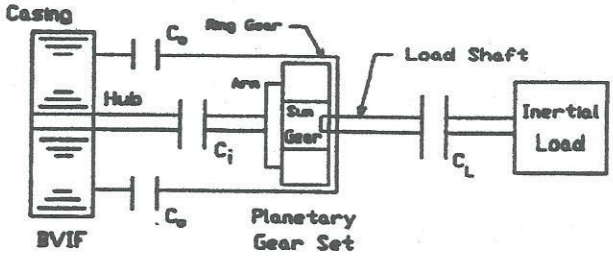

Figure 5 - The BVIF and planetary gear set arrangement during the load acceleration

David G. Ullman has derived and presented the dynamic equation of motion for this particular system [13]. For convenience, the three basic nonlinear differential equations representing the dynamic equations of motion of the system are presented here:

$$T_i + T_b = \frac{d}{dt}(I_i\omega_i) \qquad (7)$$

$$T_o - T_b = \frac{d}{dt}(I_o\omega_o) \qquad (8)$$

The relations for the moments of inertias I_i, and I_o are:

$$I_i = \frac{\pi\rho b}{2}\left(r_2^4 - r_1^4\right) + I_{if} \qquad (9)$$

$$I_o = \frac{\pi\rho b}{2}\left(r_4^4 - r_3^4\right) + I_{of} \qquad (10)$$

where ρ and b are the band material density and width. The term r_1 and I_{if} are the radius and the fixed inertia of the inner hub, while r_4 and I_{of} are the inner radius and the fixed inertia of the outer casing respectively.

In Equations (7) and (8), the term T_b is the torque applied to the flexible band in the following form:

$$T_b = \frac{1}{2}nh\rho b\frac{r_2 r_3}{r_3 - r_2}\left[r_3^2\omega_o^2 - r_2^2\omega_i^2\right] \qquad (11)$$

where:

n = number of bands
h = band thickness

In addition to the differential equations of motion (Equations 5 and 6), the time rate of change of the band position wrapped around the inner hub, r_2, may be defined as follows [12]:

$$\dot{r}_2 = \frac{nhr_3(\omega_o - \omega_i)}{2\pi(r_3 - r_2)} \qquad (12)$$

Equations (7) through (12) describe the dynamic behavior of the BVIF system.

The term T_i and T_o represent the external torques applied to the inner hub and the outer casing respectively, and are given in the following forms [15]:

$$T_i = -\frac{1}{1 - gr_a} T_L \qquad (13)$$

$$T_o = \frac{gr_a}{1 - gr_a} T_L \qquad (14)$$

Here, gr_a indicates the ratio of the inner hub angular rate, ω_i, during the acceleration phase of the load to the casing angular rate ω_o, when the load shaft is stationary. The term T_L is the applied load torque and has the following relation:

$$T_L = I_L\dot{\omega}_L + T_f + T_{ad}\omega_L^2 \qquad (15)$$

where, the terms T_f and $T_{ad}\omega_L^2$ indicate the coulomb friction and aerodynamic resistance torques on the load.

The load angular velocity is related to the inner hub and outer casing angular rate through the interconnection of the planetary gearing. This relation is given as:

$$\omega_L = \frac{1}{1 - gr_a}\omega_i - \frac{gr_a}{1 - gr_a}\omega_o \qquad (16)$$

The Fourth-Order Runge-Kutta technique [16] is used to evaluate the output characteristics of the BVIF system due to high nonlinearity of the system's dynamic equations of motion, Equations (7) through (13).

The BVIF system powering an inertial load must accomplish three tasks: the load must first be accelerated, then cruised for a desired period of time, after which it is slowed down. However, this acceleration takes place by means of a different planetary gearing arrangement within the BVIF than does the acceleration. The selection of an appropriate gear ratio for the epicyclic gear train connecting the elements of the BVIF would fulfill this requirement.

To fulfill the above task, the ring gear of the planetary is connected to the load, while the sun gear is connected to the inner hub. Deceleration is accomplished by disengaging all components of the BVIF and the planetary gear set in the acceleration state and reengaging them in the manner shown in Figure 6.

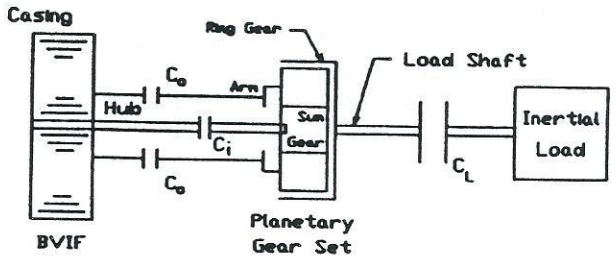

Figure 6 - The BVIF and planetary gear set arrangement during load deceleration

The governing dynamic equations of motion of the system remains the same for both acceleration and deceleration, except for the kinematic relationship which exists between the components of the BVIF and the inertial load being decelerated. The load angular speed can then be derived from the following expression:

$$\omega_L = -\frac{1}{gr_d}\omega_i + \frac{gr_d + 1}{gr_d}\omega_o. \qquad (17)$$

where, gr_d is the ratio of the input angular speed (sun gear) to the output angular speed (ring gear) during the deceleration of the load.

The torques applied to the inner hub, T_i, and outer casing, T_o, are related to the load torque through the following relations:

$$T_i = \frac{1}{gr_d} T_L \qquad (18)$$

$$T_o = -\frac{gr_d + 1}{gr_d} T_L. \qquad (19)$$

BVIF-Integrated Urban Transit Bus

Having discussed the characteristics of a diesel urban bus and of the BVIF system, this section describes the behavior of a BVIF-hybrid bus.

Two design problems must be addressed before the BVIF system can successfully be utilized as an assistant energy storage for the urban transit bus.

First, the geometric dimensions of the BVIF have to be scaled up from the experimental model [13] without the loss of the generality of the system's behavior. Secondly, the resulting prototype-size BVIF must be so configured that it will be able to accelerate an actual vehicle from rest to a desired speed at least as well as a conventionally-powered vehicle under standard road and traffic condition.

In satisfying the first problem addressed above, the Buckingham π-Theorem [3] is applied to obtain the relationship between the dimensional quantities. The geometric configuration of the BVIF model can thus be scaled up to meet the power requirement of the transit bus.

Design Consideration for Integrating the BVIF into the Urban Bus

A flywheel in a moving vehicle will react with a gyroscopic moment due to any angular movement of its axis of rotation. This gyroscopic moment is due to the flywheel spinning about one of its principal axes of inertia with a prescribed angular velocity, while the same axis of rotation moves relative to a Newtonian fixed frame of reference.

Among the three alternative designs proposed [3], to place the BVIF into a transit bus, the most feasible and efficient proves to be that in which the BVIF is placed between the vehicle's transmission and the rear axle shaft. Figure 7 shows a schematic of this design.

Once chosen as the study design, the geometric parameters of the BVIF design were scaled up to conform to the vehicle requirements. Through a number of computer simulation runs, the gear ratio of the bevel gear interconnecting the vehicle driveshaft and the BVIF load shaft was selected, as were numerical values for the parameters constructing the BVIF geometric form [3].

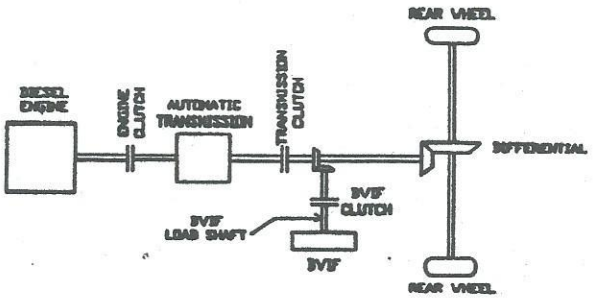

Figure 7 - The BVIF-integrated bus design

Control System Strategy

The automatic control system which performs the task of incorporating the BVIF into its transit bus is primarily of the logic control (on-off) form [17]. The operation of such an automatic process may be thought of in terms of a sequence of interrelated logic statements, similar to those used in computer programming. In this study, the control logic is simply built into the computer simulation program as are described in the followings.

Illustrated in Figure 8, the control system permits a fully sensing of the vehicle motion and selectively interconnects the elements of the system at three different modes of operation: acceleration, cruise, and deceleration. Prior to acceleration of the vehicle, the flywheel is fully charged through connecting the BVIF load shaft to the engine shaft. A slight pressure on the accelerator pedal causes the BVIF clutch sensor A and the driveline clutch sensor to activate, engaging the BVIF load shaft and the driveline shaft to the bevel gear simultaneously (Figure 8). This operation couples the stored energy source directly to the drive train, thus providing forward movement without use of the vehicle's engine.

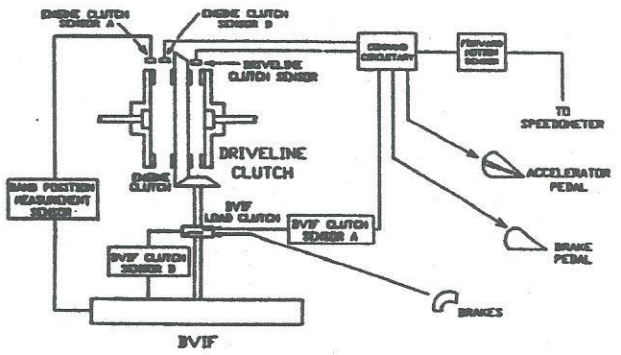

Figure 8 - Control system strategy diagram for BVIF-integrated bus

During this process, the vehicle's engine is disengaged from the driveline, operating at idle mode. The bus is accelerated by the BVIF alone until the level of energy in the flywheel, as measured by the energy level sensor has been depleted to a predetermined minimum. At this point, the BVIF is disengaged from the driveline by the BVIF clutch sensor B command. Immediately, the primary power source, or vehicle engine, is engaged with the driveline through the engine clutch sensor A to allow a continuous forward motion of the vehicle.

The bus is cruised for a period of time powered by the vehicle's engine. When the vehicle is

required to stop, a slight touch on the brake pedal sends a signal through the command circuitry, causing the engine clutch sensor B to automatically disconnect the engine from the driveline. Simultaneously, the BVIF clutch sensor A engages the BVIF load shaft, this time with the planetary gear arrangement for deceleration, to the drive train. This new arrangement with the BVIF planetary gear set bears to the load now causes the vehicle to slow down, while allowing the braking energy, normally dissipated, to accumulate in the flywheel.

Due to the relative angular rates of the inner hub and the outer casing for the planetary set gear ratio, the band starts to wind out from inside of the outer casing and wrap around the hub, increasing the moment of inertia associated with the inner segment of the BVIF system. When the band of the BVIF, measured from the hub shaft center, approaches its initial position prior to acceleration of the vehicle, an automatic sensor disengages the BVIF load shaft from the bus driveline. At this point, a signal is sent to the driver to apply the vehicle's friction brake to slow down the vehicle to a complete stop.

During this period, an energy level sensor measures the quantity of stored kinetic energy in the flywheel. If the level of the energy in the BVIF has not attained its initial setting prior to the vehicle's acceleration, the engine clutch sensor A automatically engages the engine to recharge the BVIF to a predetermined level.

Conventional and BVIF-Integrated Bus Simulation Results

A numerical computer simulation based on the given data [3] represents the performance of the bus over a prescribed course. The data used for the speed and the length of the dural pattern are taken from an actual survey of a typical city bus operating in a normal traffic day. The effect of the resistance road load, drag forces, and rolling friction are functions of the vehicle's speed. Changes in environmental conditions, such as the head wind velocity, and the road elevation, are omitted to simplify computation.

A typical wide-open throttle acceleration output for one cycle of motion of the conventional bus and the BVIF-integrated vehicle for the same distance of travel is shown in Figures 9 and 10.

Figure 9 represents a one-cycle acceleration, cruise, and deceleration of both vehicles as function of time. In this figure, the dashed line illustrates the time history of the conventional bus. The bus is accelerated to a speed of 32.5 miles per hour (mph) (position A_1), a typical average city bus speed, and cruised for a total of 20 seconds at the constant speed to position A_2 where it is slowed down to a complete stop by means of the vehicle's brakes. The bus deceleration, modeled as column friction, takes nearly 10 seconds. This is an average deceleration period taken from an actual bus operation in city traffic.

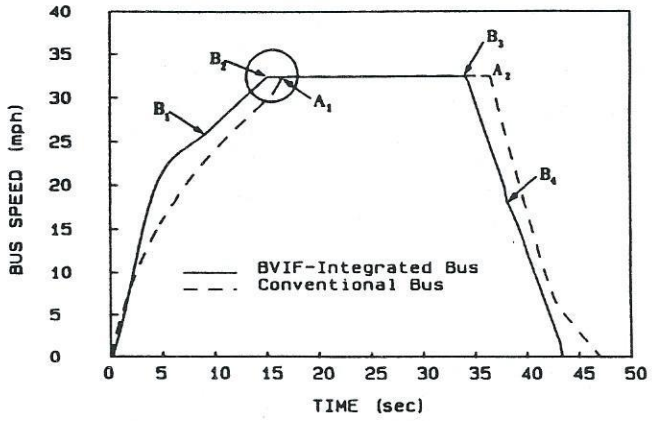

Figure 9 - The BVIF-integrated and conventional bus speed vs time

The solid line in Figure 9 shows a one-cycle operation of a BVIF-integrated bus system. As described in previous section, the fully charged BVIF is engaged to the driveline, accelerating the bus to a nearly 25 mph (position B_1 in Figure 9). At this point, the BVIF energy content reaches its minimum value, which causes the automatic control system to disengage the flywheel from the drivetrain and engage the engine to power the vehicle to a cruising speed of 32.5 mph (position B_2). The bus motion is continued at this speed for the next 20 seconds. When the vehicle reaches the point at which it must begin to decelerate (position B_3 in Figure 9), the engine is disengaged from the vehicle's drivetrain.

The BVIF load shaft then reengages to slow the vehicle down through the appropriate arrangement of the BVIF and the planetary gear system. The speed of the bus lowered to approximately 17 mph (position B_4); the band position around the inner hub of the BVIF has once again reached its initial starting point. The flywheel is then disengaged from the drive wheels and the brakes are applied to bring the vehicle to a full stop. The total time of deceleration for the BVIF-integrated bus is slightly over 9 seconds, which is almost the same time elapsed deceleration time as that of the conventional bus.

Notice that even though there is a slight delay in the acceleration of the BVIF-integrated bus just before the engine substitute for the flywheel (position B_1) the BVIF-integrated bus reaches the

predetermined cruising speed of 32.5 mph earlier than the conventional bus. This phenomenon is highlighted by a circle in Figure 9.

Figure 10 presents an acceleration-deceleration pattern of the conventional and BVIF-integrated bus system. The dashed line is the acceleration-deceleration time history of the conventional bus. The conventional bus's initial acceleration of 7 ft/sec^2 diminishes as the vehicle speeds up and finally reaches zero when the vehicle's speed reaches a constant value. The vehicle is then slowed down through a constant deceleration to a complete stop.

The solid line in Figure 10 represents the acceleration-deceleration cycle of the BVIF-integrated bus during a start-stop motion. Through BVIF energy supply, the bus is accelerated to over 8 ft/sec^2 (position A). This acceleration diminishes as the bus speed is increased from position A to B. At the position indicated by B, the BVIF is disengaged from the driveline and engine accelerates the vehicle further to a coristant speed where the vehicle is no longer accelerating (position C). After the bus cruises for a period of 20 seconds at a steady speed, it is slowed down with a constant deceleration of -10 ft/sec^2 through the BVIF engagement to the drive train and further with the vehicle's braking. Notice that the rate of deceleration of the BVIF-integrated bus is about twice that of a conventional system. This deceleration still remains within comfortable range for the on-board passengers, since this value is less than one third of the gravitational acceleration.

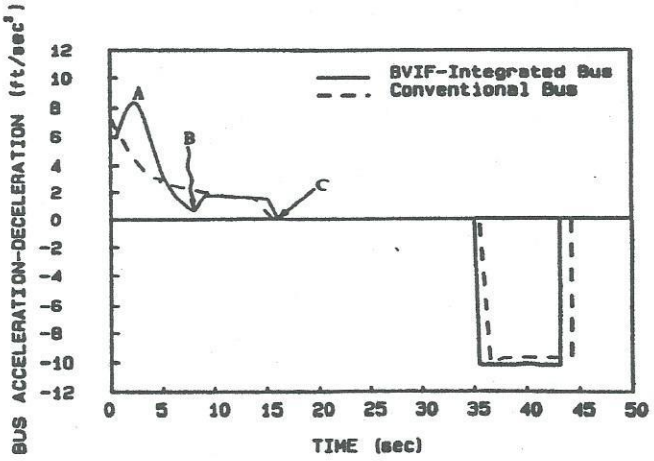

Figure 10 - The BVIF-integrated and conventional bus acceleration-deceleration vs time

Performance Comparison of the Conventional and BVIF-Integrated Bus

The performance of the conventional and the BVIF-integrated bus during several start-stop cycles are evaluated and compared [3]. These comparisons are made for both fuel consumption and brake shoe wear of the two vehicles.

Bus Fuel Economy

An analytical approach is taken to determine the fuel usage of the two vehicles in four different modes: acceleration, steady-state cruise, deceleration, and engine idling. The vehicle dural pattern fuel economy has been evaluated by computer using a method described by David N. Hwang [18]. Using this procedure, the fuel consumption of the conventional and the BVIF-integrated buses was evaluated over a course of various fixed urban driving schedules. The results are compared in Figure 11. The advantage in fuel economy of the BVIF-integrated bus over the conventional system is immediately apparent. Representing a significant cost savings for its owner/operator, the BVIF-integrated bus used over 30% less fuel than did the comparable, conventionally-powered bus.

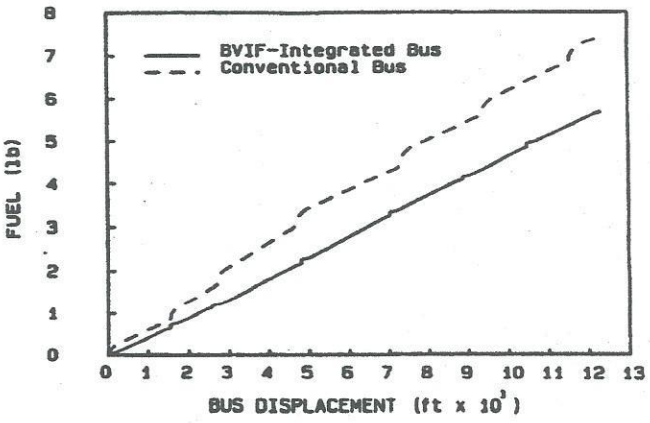

Figure 11 - Bus fuel consumption vs displacement

Brake Shoe Wear

In addition to fuel saving, the BVIF-integrated vehicle also should offer substantial economy over the conventional bus in one other important area of overall performance; the braking system. As a conventional vehicle is brought to stop, the kinetic energy of the vehicle is converted into heat which is

then dissipated wastefully into the atmosphere. In the BVIF-integrated vehicle, however, this energy is recovered to provide acceleration during the next driving cycle. Obviously, the brakes of the BVIF bus will be called upon to do far less than its conventional counterpart, a fact which should result in significantly less friction wear on its brake shoes, increased brake life, and decreased costs for brake maintenance.

Minehishi and Shimizu [19], introduced an algorithm to evaluate brake wear/life which can be applied to a vehicle in any typical driving condition. Using this method, the brake shoe wear of the conventional bus and BVIF-integrated vehicle were evaluated. The parameters used in the computer simulation study were provided by the manufacturer of the brakes [3].

The results obtained from the computer simulation of the two buses are plotted in Figure 12; they represent the relative brake shoe wear of the conventional bus (dashed line) and the BVIF-integrated bus (solid line).

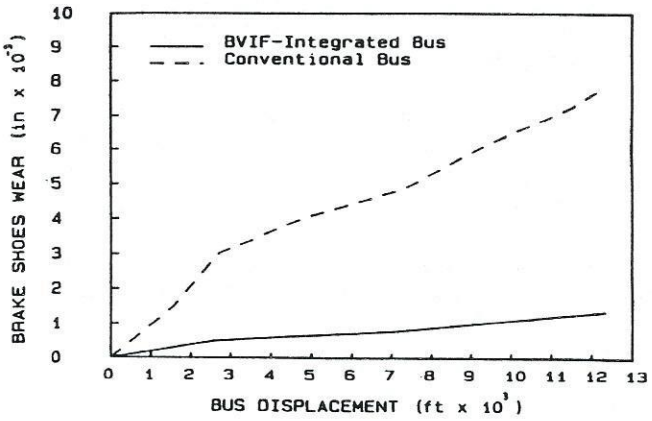

Figure 12 - Bus brake shoes wear vs displacement

The marked improvement of the brake shoe performance life on a BVIF-integrated vehicle as compared to that of conventional system is apparent from this graph. The BVIF-integrated proved the brake life by a factor of five times over the conventional system.

Conclusions

This study has demonstrated the feasibility of incorporating a new type of hybrid power system into the urban transit bus, a power system which integrates into the conventional engine and drive train an auxiliary source of energy provided by the band variable-inertia flywheel. The addition of the BVIF system makes possible the recovery of a significant portion of the energy normally expended in the fuel-efficient process of acceleration and deceleration. As determined by computer simulation, an alternative fuel saving of up to thirty percent is possible when a BVIF-hybrid system is compared to that of a conventional bus over a predetermined course of terrain.

The regenerative braking system of the BVIF-hybrid bus was shown to improve the life of the brake shoes by a factor of five, reducing the costs of replacement parts and labor for maintenance.

In addition, the BVIF system eliminates the need for the torque convertor or fluid coupling system usually installed between the engine and the automatic transmission in a conventional bus. The BVIF was demonstrated to have enough energy and power to accelerate the bus from rest to the speed at which the torque convertor normally would be locked, a period during which the torque convertor operates very inefficiently. Substitution of the BVIF for the convertor would represent further reduction in the complexity, weight, and cost of the overall propulsion system.

References

1. Data from the Engine and Transmission Manufacturer. Detroit Diesel Allison, Division of General Motors. Indianapolis, Indiana, 1986.

2. Palm III, W. J., Modeling, Analysis, and Control Dynamic Systems, John Wiley and Sons, Inc., 1983.

3. Moosavi-Rad, H., "The Application of a Band Variable-Inertia Flywheel to an Urban Transit Bus", Ph.D. Dissertation, Oregon State University, March 1988.

4. Ullman, D. G., "The Band Type Variable Inertia Flywheel and Fixed Ratio Power Recirculation Applied to it", Presented at the Mechanical and Magnetic Energy Storage Technology Meeting, October 1978.

5. Schilke, N. A., DeHart, A. O., Hewko, L. O., Mathews, C. C., Pozniak, D. J., Rohde, S. M., "The Design of an Engine-Flywheel Hybrid Drive System for a Passenger Car", Proceeding of Institution of Mechanical Engineers, Vol. 200, No. D4, 1986.

6. Beachley, N. H., and Frank, A. A., "Improving Vehicle Fuel Economy with Hybrid Power System", SAE Paper 780667, 1978.

7. Frank, A. A., Beachley, N. H., Harter, R. W., Dietrich, A. P., and Lau, K. C., "Continuously-Variable Transmission Concepts Suitable for Flywheel Hybrid Automobile", Proc. 12th Intersociety of Energy Conversion Engineering Conference.

8. Iwatsuki, T., Shimizu, K., Yano, T., "Control of CV Transmission for Internal Combustion Engine/Flywheel Hybrid Vehicle", Proc. of the 20th Intersociety Energy Conv. Eng. Conf., Published by SAE (P-164), Warrendale, PA, USA, 1985.

9. Frank, A. A., and Beachley, N. H., "Design Consideration for Flywheel-Transmission Automobile", SAE Paper 800886, 1980.

10. Ullman, D. G., "A Variable Inertia Flywheel as an Energy Storage System", Ph.D. Dissertation, Ohio State University, March 1978.

11. Ullman, D. G., and Velkoff, H. R., "An Introduction to the Variable Inertia Flywheel, VIF", Journal of Applied Mechanics, Vol. 46, No. 1, March 1979.

12. Ullman, D. G., "Preliminary Development of the Band Type Variable Inertia Flywheel (BVIF), Final Report", Prepared for Sandia Laboratories under Contract 07-3661, November 1979.

13. Ullman, D. G., and Corey, J., "Continued Development of The Band Variable Inertia Flywheel, Final Report", Union College, Schenectady, New York, 1980.

14. Ullman, D. G., and Corey, J., "The Accelerating Flywheel", 1980 Flywheel Technology Symposium, October 1980, Scottsdale, Arizona, pp. 268-286.

15. Freguson, R. J., "Short Cuts for Analyzing Planetary Gearing", Journal of Machine Design, May 26, 1983.

16. James, M. L., Smith, G. M., and Wolford, J. C., Applied Numerical Method for Digital Computation with Fortran and CSMP, 2ed Edition, Harper and Row, Publishers, 1977.

17. Doebelin, O. E., Control Principles and Design, John Wiley and Sons, Inc., 1985.

18. Hwang, D. N., "Fundamental Parameters of Vehicle Fuel Economy and Acceleration", SAE Paper No. 690541, 1969.

19. Minegishi, H., Shimizu, H., Wakamatsu, H., and Yoshino, Y., "Prediction of Brake Pad Wear/Life by Means of Brake Severity Factor as Measured on a Data Logging System", SAE Paper No. 840358, 1984.

20. Rockwell International Corporation, Automotive Operation, 2135 West Maple Road, Troy, MI 1986.